Received: 7 February 2018 | Accepted: 21 November 2018
DOI: 10.1002/hyp.13360

WILEY

SPECIAL ISSUE: WATER IN THE CRITICAL ZONE

A low-dimensional model of bedrock weathering and lateral flow coevolution in hillslopes: 1. Hydraulic theory of reactive transport

Ciaran J. Harman[1,2] | Minseok Kim[1]

[1]Department of Environmental Health and Engineering, Johns Hopkins University, Baltimore, Maryland
[2]Department of Earth and Planetary Science, Johns Hopkins University, Baltimore, Maryland

Correspondence
Ciaran J. Harman, Department of Environmental Health and Engineering, Johns Hopkins University, Baltimore, Maryland.
Email: charman1@jhu.edu

Funding information
Division of Chemical, Bioengineering, Environmental, and Transport Systems, Grant/Award Number: CBET-1360415; Division of Earth Sciences, Grant/Award Number: EAR-1344664 and EAR-90072546

Abstract

This is the first of a two-part paper exploring the coevolution of bedrock weathering and lateral flow in hillslopes using a simple low-dimensional model based on hydraulic groundwater theory (also known as Dupuit or Boussinesq theory). Here, we examine the effect of lateral flow on the downward fluxes of water and solutes through perched groundwater at steady state. We derive analytical expressions describing the decline in the downward flux rate with depth. Using these, we obtain analytical expressions for water age in a number of cases. The results show that when the permeability field is homogeneous, the spatial structure of water age depends qualitatively on a single dimensionless number, Hi. This number captures the relative contributions to the lateral hydraulic potential gradient of the relief of the lower-most impermeable boundary (which may be below the weathering front within permeable or incipiently weathered bedrock) and the water table. A "scaled lateral symmetry" exists when Hi is low: age varies primarily in the vertical dimension, and variations in the horizontal dimension x almost disappear when the vertical dimension z is expressed as a fraction $z/H(x)$ of the laterally flowing system thickness $H(x)$. Taking advantage of this symmetry, we show how the lateral dimension of the advection–diffusion-reaction equation can be collapsed, yielding a 1-D vertical equation in which the advective flux downward declines with depth. The equation holds even when the permeability field is not homogeneous, as long as the variations in permeability have the same scaled lateral symmetry structure. This new 1-D approximation is used in the accompanying paper to extend chemical weathering models derived for 1-D columns to hillslope domains.

KEYWORDS
critical zone, lateral flow, saprolite hydrology, weathering

1 | INTRODUCTION

The movement of water vertically and laterally through a hillslope is both determined by its internal permeability structure and a control on the evolution of that structure (Anderson, von Blanckenburg, & White, 2007; Brantley et al., 2017). This paper and its companion (Harman & Cosans,) are concerned with understanding the feedback between the weathering of bedrock and the lateral flow of water. Weathering modifies the porosity and permeability of the rock as it weathers (Goodfellow et al., 2015), and so modifies the storage of water and the potential gradients driving its release to streams. Our interest here is not in the details of the weathering reactions or their relationship to permeability, but rather on the way this feedback might determine the internal organization of water, solutes, and minerals within hillslopes (Brantley et al., 2017; Rempe & Dietrich, 2014; Riebe, Hahm, & Brantley, 2017), and provide a mechanism by which the rate weathering fronts advance downward can become adjusted to the rate adjacent streams incise into the bedrock in tectonically uplifted areas (Ferrier, Riebe, & Hahm, 2016; Rempe & Dietrich, 2014).

Although 3-D transient reactive transport models suitable for modeling weathering exist (Steefel et al., 2014), prior modeling studies aiming to understand first-order controls on the organization of weathering fronts within hillslopes have not considered the role of lateral flow (e.g., Lebedeva, Sak, Ma, & Brantley, 2015). Simplified models can sometimes provide elegant and revealing insights into first order controls that are difficult to tease out from the results of more complex

models. Much has been learned from the application of 1D weathering models that can be solved analytically (Lebedeva, Fletcher, & Brantley, 2010; Li, Jacobson, & McInerney, 2014; Maher & Chamberlain, 2014), but such insights are more difficult to extend to the 2-D or 3-D case.

The objective of these two papers is to develop a low-dimensional model coupling lateral flow and transport in hillslopes to weathering reactions and porosity–permeability relationships, and use this model to understand basic controls on weathering in hillslopes. The model can be solved analytically or approximately in a number of interesting cases, yielding direct insights into the nature of the feedback and the particular mechanisms determining it. The second paper describes the weathering and permeability models and explores the broader issues introduced above. We will defer until then a more thorough introduction to those issues. This first paper discusses lateral flow processes in hillslopes and lays out assumptions used to simplify the groundwater flow and advection–diffusion-reaction equations.

Lateral flow is almost exclusively saturated flow. Although saturation and lateral potential gradients can extend well above the water table (e.g., Silliman, Berkowitz, Simunek, & Van Genuchten, 2002), flow in the unsaturated zone is primarily vertical, not lateral. For this reason, geochemical processes in the unsaturated zone can be treated as 1-D "pedons" (Maher, 2011), freely draining to some deeper water table. Here, we will instead focus on that deeper system, and ultimately show how (under appropriate assumptions) it too can be approximated as a 1-D vertical system from the perspective of solute transport and reaction.

We will assume that the transport of solutes produced by weathering can be modeled by the advection–dispersion-reaction equation (ADE; Logan, 2001):

$$\frac{\partial \phi C}{\partial t} = -\nabla(\vec{q}\ C) + \nabla(\phi \mathbf{D} \nabla C) + \phi R, \tag{1}$$

where C is a solute concentration, ϕ is porosity, $\vec{q}$ is the Darcy flux field, and $\mathbf{D}$ is the hydrodynamic dispersion tensor, and $R(\vec{x}, t)$ is the rate C is produced by reactions. The interaction between mechanical dispersion and effective reaction rates can be complex, and a full treatment here would introduce considerable complexity. Here, we will neglect the full description of dispersion, retaining only molecular diffusion, which is believed to play an important role in weathering reactions (Murphy, Oelkers, & Lichtner, 1989).

The Darcy flux $\vec{q}$ is determined by the 3-D distribution of hydraulic potential (pressure and elevation) and the spatial field of permeability. Within hillslopes, this field can be complex. The inputs of rainfall or snowmelt vary in space and time, with recharge to depth often believed to be vary along a hillslope (e.g., Woods et al., 1997) and in time, often with a seasonal periodicity determined by the relative timing of water inputs and transpiration demand (e.g., Lee & Kim, 2007). In addition, a host of physical and biological processes can generate preferential flow (along bedrock fractures, decayed root channels, animal burrows, frost cracks) that rapidly transports water to depth (Beven & Germann, 2013; Sidle, Noguchi, Tsuboyama, & Laursen, 2001). Here, we will neglect these complications, and instead focus on developing first-order insights that might help to frame and interpret more sophisticated treatments in the future. Indeed, a number of recent studies have begun to examine weathering reaction processes using fully spatially resolved numerical models (e.g., Bao, Li, Shi, & Duffy, 2017; Lebedeva, Fletcher, Balashov, & Brantley, 2007; Lebedeva, Fletcher, & Brantley, 2010; Lebedeva, Sak, Ma, & Brantley, 2015; Li et al., 2017).

To develop a simplified description of the processes, we will make use of the hydraulic theory of groundwater flow and consider only steady state, spatially uniform recharge. Hydraulic groundwater theory provides useful and tractable approximations predicting the position of water tables and lateral flow rates and has been the subject of extensive research (e.g., Boussinesq, 1877; Brutsaert, 1994; Troch et al., 2013). A relatively small proportion of studies have considered the implications for solute transport (e.g, Fiori, 2012; Haitjema, 1995), perhaps because of a common misconception that hydraulic theory assumes flow paths to be horizontal (or at least aligned with the lower boundary), which is not the case. Without information about the vertical component of water flux, hydraulic groundwater theory would not be able to say much about the propagation of solutes through the system.

Here, we will discuss the use of hydraulic groundwater theory for predicting flow pathways in hillslopes, and derive results illustrating the implications for reactive transport in some cases relevant to weathering in the critical zone. We will use water age as a useful proxy for visualizing the effects of hillslope-scale flow and transport on a generic reaction. For a first-order reaction, age determines reaction progress, and so, the spatial structure of age is expected to correlate with the spatial structure of the reacting species. The spatial structure of age reveals some useful spatial symmetry in certain hillslopes that can be used to simplify the problem. In the companion paper (Harman & Cosans,), we will argue that these symmetries (and the simplifications that arise from them) can carry over to certain nonlinear weathering reactions, so long as the associated boundary conditions do not "break" the symmetry.

2 | HYDRAULIC GROUNDWATER THEORY

2.1 | The Dupuit–Forcheimer assumptions and the Boussinesq equation

Hydraulic groundwater theory aims to provide a simplified description of unconfined, saturated groundwater flow in systems that are substantially larger in lateral than vertical extent. Typically, it is applied in aquifers receiving recharge from above and bounded below by an impermeable or nearly impermeable base B. The theory rests on certain simplifying assumptions that allow hydraulic gradients normal to the (semi)impermeable base to be ignored. It is sometimes suggested that these include the assumption that all flow is parallel to the base, but this is not correct. In fact, the necessary assumption is that the dissipation of total hydraulic head h (i.e., head loss due to internal viscous damping) is primarily due to lateral flow (along the slope), rather than normal flow (e.g., Haitjema, 2016). Flow normal to the base may occur, but it is not responsible for the major part of the head dissipation over the problem domain. As a result, the variation in pressure normal to the base does not significantly impact the overall shape of the water table surface. This condition can be met in an isotropic aquifer at steady state if the lateral extent of stream tubes in the domain are typically much larger than their vertical extent in

most parts of the domain. This is generally the case in topographically controlled shallow hillslope aquifers, where the saturated thickness is on the order of at least $10^1 - 10^2$ times smaller than hillslope lateral extent (from divide to stream; Gleeson, Marklund, Smith, & Manning, 2011; Haitjema & Bruker, 2005. Consequently, variations in h in the normal dimension z can be neglected in these systems. The approach is expected to perform less well where vertial gradients are steep, such as in the vicinity of a seepage face or pumping well (Bear, 1988).

Hillslope hydraulic groundwater theory has been applied to hillslopes whose (semi)impermeable surface B is horizontal, has a constant slope, or a convex/concave profile, and a plan form that may be straight, convergent, or divergent (e.g., Fan & Bras, 1998; Troch, Paniconi, & Van Loon, 2003). We will consider the specific case of a straight hillslope domain with a constant base slope, bounded by a groundwater divide (at $x = 0$) and at the toe of the hillslope by some boundary condition representing the hillslope's interaction with a stream or floodplain (at $x = L$). Figure 1 illustrates the idealized domain.

The total head at a location x (measured along the impermeable boundary) can be expressed in terms of the elevation of the lower boundary of the flowing domain B, and the height of the water column up to the free surface boundary H.

$$h(x) = B(x) + H(x)\cos\theta, \tag{2}$$

where θ is the angle, B is inclined from horizontal. The factor of $\cos\theta$ accounts for the fact that H is measured normal to the base, rather than vertically.

The upper boundary H is typically taken to be the water table (defined as the location where the pressure is atmospheric), but lateral flow through the tension-saturated capillary fringe can be extensive (e.g., Silliman et al., 2002), and so the upper boundary can be extended to a head corresponding to the air-entry pressure to account for this. Here, we will take H to mean the upper extent of the saturated zone, corresponding to the water table and capillary fringe. Flux is described by the Darcy flux vector field $\vec{q} = \{q_x, q_y, q_z\}$, which has components directed downslope parallel to the base (q_x), transversally across the hillslope (q_y), and upward normal to the base (q_z). The upward flux will be negative in much of what follows, since flow is downward (thus $-q_z$ is a positive number), and $q_y = 0$ since the hillslope is assumed to be straight (neither converging nor diverging). Under the assumptions of hydraulic groundwater theory, the lateral component q_x of the Darcy flux vector $\vec{q}$ is given by (Childs, 1971):

$$q_x = -K\left(\frac{\partial H}{\partial x} - \tan\theta\right)\cos\theta. \tag{3}$$

The horizontal components are invariant in the z direction if the aquifer is homogeneous.

2.2 | Flow paths in a homogeneous hillslope aquifer

The hydraulic theory makes definite predictions about flow paths through the saturated zone for the case of a homogeneous aquifer under steady recharge r. Flowpaths originating at the water table must descend below the water table and make room for recharge entering further downslope. Consequently, both the horizontal and vertical components can be obtained from continuity (mass balance) if $H(x)$ is known.

The horizontal component of the flux is obtained simply by equating the recharge upslope of a point x to the lateral flow at that point, so $rx = q_x(x)H(x)$ (e.g., Strack, 1984; Vogel, 1966). This can be rearranged to give:

$$q_x(x) = r\frac{x}{H(x)}. \tag{4}$$

An expression for q_z can be obtained from the continuity equation, which at steady state requires:

$$\frac{\partial q_x}{\partial x} + \frac{\partial q_z}{\partial z} = 0. \tag{5}$$

Differentiating (4) with respect to x, and substituting the result into (5) yields:

$$\frac{\partial q_z}{\partial z} = -\frac{q_x}{x}\left(1 - x\frac{H'(x)}{H(x)}\right). \tag{6}$$

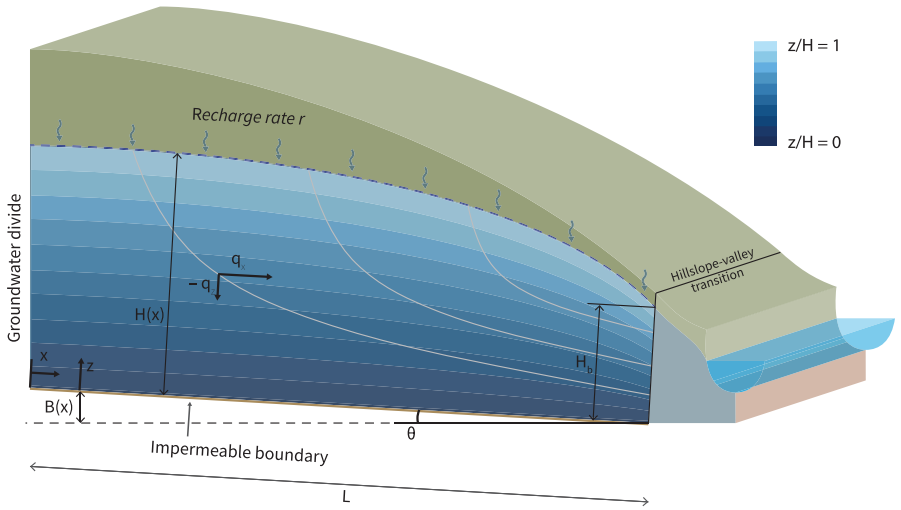

FIGURE 1 A vertically exaggerated cross section of the idealized hillslope groundwater system considered here, and the symbols used to refer to it. The lower boundary $B(x)$ is assumed to be straight, planar, and impermeable, and recharge is spatially and temporally constant rate at rate r. The blue contours within the water table show the location of constant values of the scaled vertical coordinate $Z = z/H$

Since the right hand side is a constant with respsect to z, this equation shows that the vertical component of the flux varies linearly (Strack, 1984; Streltsova, 1975). It is highest at the water table where $-q_z = r - q_x H'(x)$, and $q_z = 0$ at the impermeable base (e.g., Bear, 1988). The term in parentheses modifies the vertical flux to account for increases or decreases in the thickness of the saturated flow downgradient.

We can also obtain these results by considering a streamline extending downslope of a point x_0. If we assume a unit width of hillslope, the total recharge upslope of the point is $x_0 r$. Since all that water must be transmitted downslope, $x_0 r = H(x_0) q_x(x_0)$. Further downslope, the recharge originating from upslope of x_0, is confined to the region under the streamline originating at x_0, while recharge entering further downslope of x_0 is above the streamline. If the streamline passes through an elevation $z = z_s(x, x_0)$ at location x, the total flux below this streamline must therefore be $x_0 r = z_s(x, x_0) q_x(x)$, while above the streamline, it is $(x - x_0)r = (H(x) - z_s(x, x_0)) q_x(x)$ (e.g., Strack, 1984). Combining these by eliminating r shows that the streamlines vary hyperbolically as a proportion of total thickness $H(x)$:

$$z_s(x, x_0) = H(x)\frac{x_0}{x}. \tag{7}$$

Differentiating this with respect to x, setting $dz_s/dx = q_z/q_x$, eliminating x_0, and taking the derivative with respect to z, we can obtain the same result as in Equation 6.

2.3 | Flow paths in a heterogeneous hillslope aquifer

The situation becomes more complex if the assumption of homogeneous K is relaxed, but a useful result can still be obtained. In particular, we are interested in the case where K varies as a function of a scaled vertical coordinate, $Z(x, z) = z/H(x)$. This assumption will be justified and used later in Section 3.

Let us assume $K = K(x, Z)$, allowing (for the moment) an arbitrary conductivity field. At steady state, upslope recharge must balance and downslope Darcy flux, so $rx = \int_0^H q_x \, dz$. Using Darcy's law under the Dupuit assumptions (3), we can obtain:

$$q_x(x, Z) = r\frac{x}{H(x)}\frac{K(x, Z)}{\overline{K}(x)}, \tag{8}$$

where $\overline{K}(x) = \int_0^1 K \, dZ$ is a vertically averaged conductivity.

Taking the derivative of this with respect to x and using continuity (5) to eliminate $\partial q_x/\partial x$ yields:

$$\frac{\partial q_z}{\partial z} = -\frac{q_x}{x}\left(1 - x\left(\frac{H'(x)}{H(x)}\left(1 + Z\frac{\partial K/\partial Z}{K}\right) + \frac{\partial \log(K/\overline{K})}{\partial x}\right)\right). \tag{9}$$

This provides a generalization of (6) and reduces to it when K is constant. Let us assume that K only varies in the Z direction. That is, K may vary in x if the vertical dimension z is held constant, but does not vary if Z is held constant instead. Setting the x-derivatives to zero gives:

$$\frac{\partial q_z}{\partial z} = -\frac{q_x}{x}\left(1 - x\left(\frac{H'(x)}{H(x)}\left(1 + Z\frac{K'(Z)}{K}\right)\right)\right), \tag{10}$$

which allows the effect of this type of layering to be accounted for when computing fluxes and flow paths.

These results show that we need only derive (or observe) the steady state recharge rate and elevation of the upper surface $H(x)$ to determine both the q_x and q_z components of the entire flux field. This result arises from the kinematics imposed by mass balance and the position of the water table. However, to predict $H(x)$, we must further invoke Darcy's Law.

2.4 | Storage and flux in hillslope aquifers

The two terms in the parentheses in Equation (3) represent the contributions of the two gradients driving flow: the gradient in the thickness of the aquifer and the gradient of the underlying impervious surface B. The first of these has the form of a diffusion term, tending to smooth out steep gradients in the saturated thickness, while the second acts like an advection term, translating variations in saturated thickness downslope without transforming them.

The relative importance of these two terms determines the character of the hillslope hydraulics. The hillslope number Hi is a dimensionless number that captures their relative importance (Brutsaert, 2005):

$$\mathrm{Hi} = \frac{L\tan\theta}{\overline{H}}, \tag{11}$$

where $L\tan\theta$ is the relief of the hillslope (really the relief of the base surface B), and $\overline{H}$ is an effective thickness of the aquifer. This is approximately the average thickness (Appendix A gives a practical approximation for this). This quantity appears in derivations of analytical solutions predicting storage and flow in hydraulic groundwater theory (e.g., Brutsaert, 1994) where it has also been called the Hillslope Peclet number (Berne, Uijlenhoet, & Troch, 2005; Lyon & Troch, 2007). Under unsteady conditions, Hi has been found to be useful when $\overline{H}$ is replaced by a mean or effective aquifer thickness (e.g., Brutsaert, 1994; Harman & Sivapalan, 2009a).

When $\mathrm{Hi} \ll 1$ larger than the relief of B, and the saturated thickness gradients play an important role in determining the storage and flux of water in the landscape. When $\mathrm{Hi} \gg 1$, the relief is larger, and saturated thickness variations are less important — the topography of the underlying (semi)impermeable surface dominates. For example, a 1-m thick aquifer within a hillslope of 250-m length in a mountainous area with a slope of 30 degrees would give $\mathrm{Hi} = 144$. A 100 m hillslope of 2 degrees with a 5-m thick aquifer would have $\mathrm{Hi} = 0.7$.

Hydraulic groundwater theory gives analytical solutions for the saturated thickness $H(x)$ for the limiting cases of small and large hillslope number. When $\mathrm{Hi} \sim 0$ (Boussinesq, 1877):

$$H(x) = \sqrt{H_b^2 + H_d^2\left(1 - \frac{x^2}{L^2}\right)}, \tag{12}$$

where $H_d = L\sqrt{r/K}$ is the maximum thickness of the saturated thickness at the groundwater divide if $H_b = 0$. When $H_b \gtrsim H_d$, the saturated thickness becomes relatively uniform.

When $\mathrm{Hi} \gg 1$, the saturated thickness simply reflects the accumulation of water down the slope. The downstream boundary condition becomes less important and the saturated thickness approaches the linear relationship (e.g., Troch, van Loon, & Hilberts, 2002):

$$H(x) = \frac{xr}{K\sin\theta}. \tag{13}$$

Approximate solutions can also be found for the more general case where Hi $>$ 0 (see Appendix A).

3 | REACTIVE TRANSPORT IN A HILLSLOPE AQUIFER

3.1 | 2-D advection–diffusion-reaction

With this framework in place, we can consider the nature of reactive transport through a hillslope aquifer. This will lead to a novel expression of simplifed reactive transport in such systems. In two dimensions, the ADE (1) becomes:

$$\frac{\partial(\phi C)}{\partial t} = -q_x \frac{\partial C}{\partial x} - q_z \frac{\partial C}{\partial z} + D_m \left(\frac{\partial^2(\phi C)}{\partial x^2} + \frac{\partial^2(\phi C)}{\partial z^2} \right) + \phi R, \quad (14)$$

where D_m is the molecular diffusion coefficient, and we have used continuity under steady flow to eliminate derivatives of q_x and q_z.

We can simplify this equation by considering the relative importance of each term in the context of hillslope-scale flow and transport. We can do this by expressing the vertical and horizontal dimensions relative to the mean thickness $\overline{H}$, and hillslope length L, respectively, as $z = z'\overline{H}$ and $x = x'L$, and time relative to the mean turnover time of the aquifer $t = t'r/(\overline{H}\phi)$. Using these, the ADE becomes:

$$\frac{\partial(\phi C)}{\partial t'} = -v_x' \frac{\partial C}{\partial x'} - v_z' \frac{\partial C}{\partial z'} + \mathrm{Pe}^{-1} \left(\frac{\overline{H}^2}{L^2} \frac{\partial^2(\phi C)}{\partial x'^2} + \frac{\partial^2(\phi C)}{\partial z'^2} \right) + \frac{\overline{H}\phi}{r} R, \quad (15)$$

where v_x' and v_z' are dimensionless forms of the pore velocity, and Pe$= \overline{H}r/(D_m\phi)$ is a Peclet number. The new coordinates x', z', and t' will have magnitudes on the order of unity for hillslope-scale problems. The factor of $\overline{H}^2/L^2$ multiplying the horizontal diffusion term will be very small in hillslope problems, suggesting that in hillslope weathering reactions, the horizontal diffusion term is likely to be much less important than the vertical. In addition, since weathering products must be produced in solution all along the hillslope from ridge to toe, concentration gradients will be largely in the vertical direction, and less so in the horizontal. Horizontal advection is therefore likely to be much more important than horizontal diffusion, and the horizontal diffusion term can therefore be neglected.

In the homogeneous case, the advective terms can be further simplified by expressing them in terms of age rather than location. This is done first by substituting in Equations 4 and 6 (integrated in z) for q_x and q_z. We then change the coordinates system from the Cartesian coordinates $C(x, z, t)$ to a coordinate system based on the flow lines $C(x_0, Z, t)$, where $x_0 = xz/H(x)$ is the x coordinate of the origin of the flow path passing through (x, z) (as per Equation 7), and $Z = z/H(x)$ is the vertical location scaled by the total saturated thickness. If diffusion is neglected, the equation then simplifies to:

$$\frac{\partial C}{\partial t} - \frac{rZ}{\phi H(x_0/Z)} \frac{\partial C}{\partial Z} = R, \quad (16)$$

If we define the effective vertical velocity as $v_Z(Z) = -\frac{rZ}{f}(\phi H(x_0/Z))$, then the left hand side of this equation has the form of a material derivative along the streamline initiating at x_0. The age of a parcel of water $T = T(x_0, Z)$ can be obtained by integrating $1/v_Z$ from the point where it enters $(x, Z) = (x_0, 1)$ down to its present location:

$$T(x_0, Z) = \int_Z^1 \frac{1}{v_Z(\zeta)} d\zeta = \int_Z^1 \frac{\phi H(x_0/\zeta)}{r\zeta} d\zeta. \quad (17)$$

Note that since $t = t_0 + T$ (the current time is the sum of the time a parcel entered and its age), then the left hand side of (16) can be seen as the result of applying the chain rule to a concentration field $C(x_0, T, t_0)$ specified in terms of age T rather than Z:

$$\frac{\partial t}{\partial T}\frac{\partial C}{\partial t} + \frac{\partial Z}{\partial T}\frac{\partial C}{\partial Z} = \frac{dC}{dT} = R. \quad (18)$$

Thus, the concentration $C(x_0, T, t)$ can be obtained by simply integrating the reaction rate along a streamline:

$$C(x_0, T, t_0) = C(x_0, 0, t_0) + \int_0^T R \, d\tau, \quad (19)$$

where the first term on the right hand side is the initial concentration of the recharge. This gives the concentration field for arbitrary saturated thickness $H(x)$ and spatially variable source/sink R. Equation (19) allows us to evaluate the distribution of water age T by setting $R = 1$/day (so the "amount" of age represented by C increases by 1 day per day), and $C(x_0, 0, t_0) = 0$.

3.2 | Illustrative examples of water tables and age distributions

Below, we consider three asymptotic cases for which exact analytical solutions for water age can be obtained by integrating (17). Three examples that represent or approximate these cases are illustrated in Figure 2. In each, water tables and flow paths are shown for three hillslope aquifers, each $L = 100$-m long, with conductivity $K = 0.1$ m/day, porosity 0.15, and recharged at a rate of $r = 100$ mm/year. One has a flat lower boundary, so Hi $= 0$, and the saturated thickness at the toe is set to $H_b = 1$ m. In the other two cases, the thickness at the toe is set to 5.2 m, which is approximately the value of H_d in all three cases. The second case has a base slope of 2%, and a resulting Hi $= 0.3$, while the third has a base slope of 10%, and Hi $= 2.5$.

Uniform thickness (Hi $\ll$ 1, $H_b \gtrsim H_d$): When H is approximated as constant, the integral in (17) can be solved exactly to give (Vogel, 1966):

$$T = -\frac{\phi H}{r} \log Z. \quad (20)$$

The age distribution varies only in the vertical and not down the hillslope. The ages stack like pancakes, with the pancakes thickest at the top, and squeezed thinner and thinner at the bottom. This situation is most closely approximated when Hi is small and H_b is not so small that it causes the aquifer to pinch out at the downslope end (the middle case shown in Figure 2 illustrates this pinching effect).

Thickening upslope (Hi $\ll$ 1, $H_b < H_d$) : If we assume $H(x)$ is given by (12), the solution is slightly more complex, and is a function of Z and H at the initial and current locations:

$$T(x_0, Z) = -\frac{\phi H^*}{r} \left(\log Z + \psi(x_0, Z) \right), \quad (21)$$

where

$$\psi(x_0, Z) = \frac{H(x_0) - H(x)}{H^*} - \log\left(\frac{H(x_0) + H^*}{H(x) + H^*} \right), \quad (22)$$

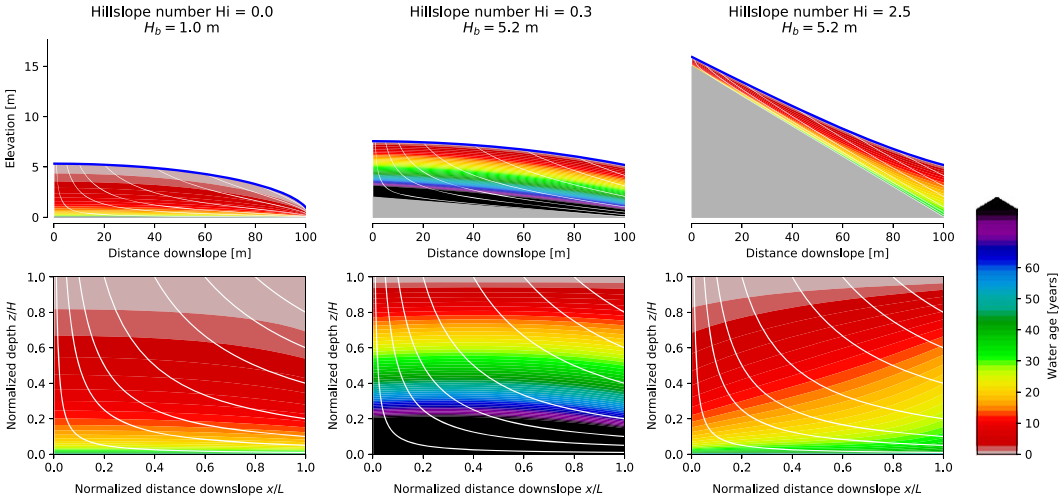

FIGURE 2 The spatial organization of water age in saturated hillslope aquifers and its dependence on the Hillslope Number, Hi. Plots A–C show the water table and age distribution with 4× vertical exaggeration. Plots D–F show the same age distribution, but with the vertical and horizontal axes scaled by $H(x)$ and L, respectively. The grey area represents impermeable bedrock. While lines are flow paths predicted by conservation of mass (see Section 2.2). When Hi < 1, the age structure varies mainly with z/H, and not with x. The same is not true with Hi > 1

with $H^* = \sqrt{H_b^2 + H_d^2}$ and $H(x) = H(x_0/Z)$. This correction term ψ turns out to be very small for much of the domain, and the age distribution is still well approximated by setting $\psi = 0$. In that case, the situation is similar to the previous case, but rather than stacking like pancakes, the ages vary in z as a proportion of the saturated thickness $H(x)$. This case can be seen in the left case of Figure 2, which is similar to the centre plot in having roughly horizontal isochrones, although the mean of the age distribution in storage is less.

Thickening downslope (Hi ≫ 1) : When the aquifer thickness varies linearly with distance downslope, the age distribution is (e.g., Cook & Böhlke, 2000):

$$T(x,z) = \frac{\phi(H(x) - z)}{r}. \tag{23}$$

Water age in this case varies only as a function of depth below the water table, $H(x) - z$. However ,since the saturated thickness is increasing downslope, this implies that the age of the water at the impermeable boundary is increasing downslope. The right case in Figure 2 approximates this behaviour. A more general approximate solution for Hi > 0 is provided in Appendix A.

3.3 | 1-D advection–diffusion-reaction with scaled lateral symmetry

Based on the results above, we can surmise that when Hi < 1, the solution to the ADE (14) depends largely on a vertically scaled coordinate $Z = z/H(x)$ and much less on x. We can therefore approximately account for horizontal fluxes using a 1-D version of the ADE that only contains derivatives in the Z direction. The resulting equation is:

$$\frac{\partial(\phi C)}{\partial t} = -q_z^* \frac{\partial C}{\partial z} + D_m \frac{\partial^2(\phi C)}{\partial z^2} + \phi R, \tag{24}$$

where:

$$\frac{\partial q_z^*}{\partial z} = -\frac{q_x}{x}. \tag{25}$$

The derivation of this is given in Appendix B. The lateral flux q_x in the equations above can be obtained from the hydraulic approximation to Darcy's Law, which we can write for convenience as:

$$q_x = -K\nabla h, \tag{26}$$

with $\nabla h = H'(x)\cos\theta - \sin\theta$ representing the lateral gradient of total hydraulic head.

4 | DISCUSSION

Equaitons 24, 25, and 26 provide a parsimonious description of flow and solute transport in an aquifer with scaled lateral symmetry in K. The derivation of these is the primary purpose of this paper, as they are the foundation for the analysis in Part 2.

This derivation is largely built on hydraulic groundwater theory, which has an extensive literature (see for example Troch et al. (2013)). Much of what is presented above is not new, and more detailed treatments can be found in the citations provided. The main results related to the concept of scaled lateral symmetry (Sections 3.3 and 2.3) are the original theoretical contributions of this work.

However, the results above also illustrate some important issues and qualitative features of lateral flow relevant for understanding weathering in hillslopes. These are discussed below. They are features of a highly idealized hillslope, and so should be viewed with an appropriate degree of skepticism. However, they will likely be recapitulated in spatially resolved numerical models that adopt broadly similar assumptions (Lebedeva et al., 2010; Li et al., 2017). Hydraulic groundwater theory in general, and the theory developed here in particular, will therefore be useful for framing hypotheses to be tested by numerical experiments. It will be particularly interesting to explore how weathering proceeds differently under high and low Hillslope number Hi.

4.1 | Flow paths and the importance of the Hillslope number Hi

There are qualitative differences between the Hi < 1 and Hi > 1 cases in the arrangement of flow paths relative to the impermeable boundary *B* (Figure 2). In both cases, only water that recharges near the ridge approaches the vicinity of the lower boundary of the system. If the lower boundary of the aquifer is the site of the majority of the weatherable material, the majority of the flow will not directly participate in the weathering reaction. However, for cases where Hi > 1, water does not even move significantly closer to the lower boundary as it travels through the hillslope, and instead primarily travels downslope. The accumulation of recharge downslope is accommodated by an increase in saturated thickness. By contrast, when Hi < 1, the accumulation of recharge is accommodated primarily by an increase in the lateral flow rate downslope.

This difference is significant. A region of weatherable material located in a strip above and parallel to *B* will receive more flow from upslope if Hi > 1 than if Hi < 1. In the former case, it will likely therefore tend to weather along its length from upslope to downslope, whereas in the latter case, it may weather more from top to bottom. Interestingly, this may tend to flatten the gradient of the strip in the Hi > 1 case. These speculations could be tested in a numerical model, and against field observations.

There are further important differences between the Hi > 1 and Hi < 1 cases under unsteady conditions, many of which have been explored in literature (e.g., Berne et al., 2005). The boundary condition at the toe of the hillslope (representing the connection to the riparian zone) does not significantly affect the storage and release of water from the hillslope if Hi is large, but does if it is small (Harman & Sivapalan, 2009a). Spatial heterogeneity in permeability within the hillslope (such as might be generated by the presence of large corestones or variable lithology) can drive variations in the water table that reroute the flow around low permeability areas if Hi is small, but the capacity to do so is more limited if it is large (Harman & Sivapalan, 2009b). This affects both the rate and age structure (residence time and transit time) of water released by heterogeneous hillslopes subject to variable recharge rates (Harman & Sivapalan, 2009b). It is not immediately clear what the implications of these differences are for weathering, or how weathering might tend to drive Hi in one direction or another as it modifies the position of the lower boundary *B*.

4.2 | The lower boundary *B* and boundary condition H_b

The results also demonstrate the importance of the downslope boundary condition for the Hi $\ll$ 1 case. The thickness of the left and centre cases in Figure 2 differ by a factor of two, and there is much more relief in the water table in the left case ($\approx$ 4 m) than the centre ($\approx$ 1 m).

The physical meaning of H_b is tied directly to that of *B*. For example, the left plot in Figure 2 might represent the case where *B* is impermeable unweathered bedrock, and the water table perched in the saprolite above this bedrock steepens and thins towards a seepage face of thickness H_b in the stream bank. The centre plot could represent the case where bedrock is highly permeable or fractured down to some depth below the stream, and lateral flow occurs through a much larger thickness of saturated material. Rather than being a material boundary, it is possible that the circulation of saturated flow and the hydraulic gradients are coupled to a larger regional flow system, and *B* represents the lower extent of the local flow cell (Toth, 1963).

In practical applications of this theory, it may be difficult to empirically determine an appropriate location for *B* and depth for H_b. Age dating tracers may be of some help in identifying the appropriate storage of water so long as the recharge rate is known, although to convert that value into a physical location for *B* and H_b an effective porosity will also be required.

4.3 | Scaled lateral symmetry and effects of dispersion

It is important to consider the conditions that must be placed on *R* and the boundary fluxes for the scaled lateral symmetry assumption to be valid. The assumed concentration of *C* at the recharge boundary must be spatially invariant. *R* does not need to be spatially invariant, but it must vary only in $Z = z/H$ for scaled lateral symmetry to hold. If *R* "breaks" the symmetry in some sense, Equation (24) will no longer hold. This may occur if *R* depends on other spatially varying or temporally varying quantities that do not follow the same symmetry.

We have also neglected the effects of hydrodynamic dispersion or macrodispersion. There are two reasons why including dispersion would substantially complicate the analysis. First, dispersion is not isotropic. Longitudinal dispersion is typically an order of magnitude larger than transverse, and the dispersion term must be treated as a tensor, not a scalar (Whitaker, 1999). However, we can conjecture that moderate dispersion would not interrupt the scaled lateral symmetry, so long as the dispersion length scale is relatively small compared with the (vertical) dimension of the domain. Theoretical analysis (Eldor & Dagan, 1972, especially their Figure 9b) supports this argument. Second, dispersion can introduce departures from idealized "well-mixed" conditions at the sub-Darcy scale that modify the effective rate laws describing the chemical reactions. This is because dispersion does not refer to the true intermingling of fluids of distinct concentrations necessary for reactions, only to the approximate colocation of fluids that may be segregated at scales smaller than we wish to resolve (for an overview of these issue, see Dentz, Le Borgne, Englert, and Bijeljic (2011)). There are observations to suggest this is true even for pore-scale dispersion effects (Gramling, Harvey, & Meigs, 2002), as well as for macrodispersion associated with spatially variable conductivity fields (Luo, Dentz, Carrera, & Kitanidis, 2008).

It is likely that heterogeneity in hydraulic conductivity has important effects on effective weathering rates at the hillslope scale (see e.g., Jung and Navarre-sitchler, 2018a, 2018b), which may in turn have important implications for the internal organization of weathering and flow paths in hillslopes. However, it may be useful to consider those effects in the context of the overall hillslope-scale concepts being developed here. Some potential effects of heterogeneity will be discussed further in the companion paper.

5 | CONCLUSIONS

In this paper, we have demonstrated an approximate "scaled lateral symmetry" in solutions to solute transport through hillslope aquifers when the hillslope number Hi is small. Hi is small if the slope of the base of the saturated flow system does not substantially contribute to the hydraulic gradient driving lateral flow. This symmetry, illustrated by an analysis of water age distributions in the 2-D case, means that variations in the solution along the vertical dimension z up to the top of the saturated thickness H depend only on the relative location z/H and not on z alone or the location downslope x.

We have also demonstrated how this symmetry can be exploited to derive a 1-D approximation of the advection–diffusion-reaction equation describing solute transport in a saturated hillslope domain. This approximation replaces the 2-D ADE (we have neglected variations along a hillslope contour) with a 1-D vertical equation. The advective flux term in the 1-D equation is not constant, but rather is an effective vertical flux that declines as it approaches the impermeable lower boundary of the domain. The approximation can account for spatially variable reaction terms and hydraulic conductivity so long as they possess the same scaled lateral symmetry. The resulting system of independent Equations 24, 25, and 26 provide a simplified description of reactive transport through saturated hillslope aquifers.

This approximate ADE has been derived under assumptions appropriate for investigating bedrock weathering processes. In the companion paper (Harman & Cosans,), we will make use of it to investigate the effects of lateral flow on bedrock weathering reactions and the feedback engendered by the effects of weathering on the properties and structure of the flow domain. It should be noted that the analysis there is restricted to the case of small Hi. Further work is required to understand the control of lateral flow on weathering (and vice versa) in landscapes underlain by steep impermeable boundaries.

ACKNOWLEDGMENTS

The authors gratefully acknowledge the supported of National Science Foundation grants EAR-1344664, CBET-1360415, and EAR-90072546. Thanks to Susan Brantley and Daniella Rempe for the many stimulating discussions that motivated this work. Thanks also to two anonymous reviewers for helpful comments.

ORCID

Ciaran J. Harman https://orcid.org/0000-0002-3185-002X

REFERENCES

Abramowitz, M., & Stegun, I. A. (1964). *Handbook of mathematical functions with formulas, graphs, and mathematical tables*. New York, NY: Dover.

Anderson, S. P., von Blanckenburg, F., & White, A. F. (2007). Physical and chemical controls on the critical zone. *Elements*, *3*(5), 315–319.

Bao, C., Li, L., Shi, Y., & Duffy, C. (2017). Understanding watershed hydrogeochemistry: 1. Development of RT-Flux-PIHM. *Water Resources Research*, *53*(3), 2328–2345.

Bear, J. (1988). *Dynamics of fluids in porous media*. New York, NY: Dover.

Berne, A., Uijlenhoet, R., & Troch, P. A. (2005). Similarity analysis of subsurface flow response of hillslopes with complex geometry. *Water Resources Research*, *41*(9), 1–10.

Beven, K., & Germann, P. (2013). Macropores and water flow in soils revisited. *Water Resources Research*, *49*(6), 3071–3092.

Boussinesq, J. (1877). *Essai Sur La Théorie Des Eaux Courantes*. Paris: Imprimerie Nationale.

Brantley, S. L., Lebedeva, M. I., Balashov, V. N., Singha, K., Sullivan, P. L., & Stinchcomb, G. (2017). Toward a conceptual model relating chemical reaction fronts to water flow paths in hills. *Geomorphology*, *277*, 100–117.

Brutsaert, W. (1994). The unit response of groundwater outflow from a hillslope. *Water Resources Research*, *30*(10), 2759–2763.

Brutsaert, W. (2005). *Hydrology*. New York: Cambridge University Press.

Childs, E. C. (1971). Drainage of groundwater resting on a sloping bed. *Water Resources Research*, *7*(5), 1256–1263.

Cook, P. G., & Böhlke, J.-K. (2000). Determining timescales for groundwater flow and solute transport. In P. G. Cook, & A. L. Herczeg (Eds.), *Environmental tracers in subsurface hydrology* (pp. 1–30). Boston, MA: Springer US.

Dentz, M., Le Borgne, T., Englert, A., & Bijeljic, B. (2011). Mixing, spreading and reaction in heterogeneous media: A brief review. *Journal of Contaminant Hydrology*, *120-121*, 1–17.

Eldor, M., & Dagan, G. (1972). Solutions of hydrodynamic dispersion in porous media. *Water Resources Research*, *8*(5), 1316–1331.

Fan, Y., & Bras, R. L. (1998). Analytical solutions to hillslope subsurface storm flow and saturation overland flow. *Water Resources Research*, *34*(2), 921–927.

Ferrier, K. L., Riebe, C. S., & Hahm, W. J. (2016). Testing for supply-limited and kinetic-limited chemical erosion in field measurements of regolith production and chemical depletion. *Geochemistry, Geophysics, Geosystems*, *17*(6), 2270–2285.

Fiori, A. (2012). Old water contribution to streamflow: Insight from a linear Boussinesq model. *Water Resources Research*, *48*(November 2011), 1–6.

Gleeson, T., Marklund, L., Smith, L., & Manning, A. H. (2011). Classifying the water table at regional to continental scales. *Geophysical Research Letters*, *38*(5), L05401.

Goodfellow, B. W., Hilley, G. E., Webb, S. M., Sklar, L. S., Moon, S., & Olson, C. A. (2015). The chemical, mechanical, and hydrological evolution of weathering granitoid. *Journal of Geophysical Research-Earth Surface*, *121*(8), 1410–1435.

Gramling, C. M., Harvey, C. F., & Meigs, L. C. (2002). Reactive transport in porous media: A comparison of model prediction with laboratory visualization. *Environmental Science & Technology*, *36*(11), 2508–2514.

Haitjema, H. M. (1995). On the residence time distribution in idealized groundwatersheds. *Journal of Hydrology*, *172*(1-4), 127–146.

Haitjema, H. (2016). Horizontal flow models that are nots. *Groundwater*, *54*(5), 613.

Haitjema, H. M., & Bruker, S. M. (2005). Are water tables a subdued replica of the topography? *Groundwater*, *43*(6), 781–786.

Harman, C. J., & Cosans, C. L. A low-dimensional model of bedrock weathering and lateral flow co-evolution: 2. Feedbacks with permeability and bedrock relief in supply-limited landscapes, Hydrological Processes.

Harman, C. J., & Sivapalan, M. (2009a). A similarity framework to assess controls on shallow subsurface flow dynamics in hillslopes. *Water Resources Research*, *45*(1), 1–12.

Harman, C. J., & Sivapalan, M. (2009b). Effects of hydraulic conductivity variability on hillslope-scale shallow subsurface flow response and storage-discharge relations. *Water Resources Research*, *45*, W01421.

Jung, H., & Navarre-sitchler, A. (2018a). Physical heterogeneity control on effective mineral dissolution rates. *Geochimica Et Cosmochimica Acta*, *227*, 246–263.

Jung, H., & Navarre-sitchler, A. (2018b). Scale effect on the time dependence of mineral dissolution rates in physically heterogeneous porous media. *Geochimica Et Cosmochimica Acta*, *234*, 70–83.

Lebedeva, M. I., Fletcher, R. C., Balashov, V. N., & Brantley, S. L. (2007). A reactive diffusion model describing transformation of bedrock to saprolite. *Chemical Geology*, *244*(3-4), 624–645.

Lebedeva, M. I., Fletcher, R. C., & Brantley, S. L. (2010). A mathematical model for steady-state regolith production at constant erosion rate. *Earth Surface Processes and Landforms*, *35*(5), 508–524.

Lebedeva, M. I., Sak, P. B., Ma, L., & Brantley, S. L. (2015). Using a mathematical model of a weathering clast to explore the effects of curvature on weathering. *Chemical Geology*, *404*, 88–99.

Lee, K.-S., & Kim, Y. (2007). Determining the seasonality of groundwater recharge using water isotopes: A case study from the upper North Han River basin, Korea. *Environmental Geology*, *52*(5), 853–859.

Li, D. D., Jacobson, A. D., & McInerney, D. J. (2014). A reactive-transport model for examining tectonic and climatic controls on chemical weathering and atmospheric CO2 consumption in granitic regolith. *Chemical Geology*, *365*, 30–42.

Li, L., Maher, K., Navarre-sitchler, A., Druhan, J., Meile, C., Lawrence, C., ... Beisman, J. (2017). Expanding the role of reactive transport models in critical zone processes. *Earth-Science Reviews*, *165*, 280–301.

Logan, J. D. (2001). Reaction-Advection-Dispersion Equation, *Transport modeling in hydrogeochemical systems*. New York: Springer, pp. 29–73.

Luo, J., Dentz, M., Carrera, J., & Kitanidis, P. (2008). Effective reaction parameters for mixing controlled reactions in heterogeneous media. *Water Resources Research*, *44*(2), W02416.

Lyon, S. W., & Troch, P. A. (2007). Hillslope subsurface flow similarity: Real-world tests of the hillslope Peclet number. *Water Resources Research*, *43*(7), W07450.

Maher, K. (2011). The role of fluid residence time and topographic scales in determining chemical fluxes from landscapes. *Earth and Planetary Science Letters*, *312*(1-2), 48–58.

Maher, K., & Chamberlain, C. P. (2014). Hydrologic regulation of chemical weathering and the geologic carbon cycle. *Science (New York, N.Y.)*, *343*(6178), 1502–1504.

Murphy, W. M., Oelkers, E. H., & Lichtner, P. C. (1989). Surface reaction versus diffusion control of mineral dissolution and growth rates in geochemical processes. *Chemical Geology*, *78*(3-4), 357–380.

Rempe, D. M., & Dietrich, W. E. (2014). A bottom-up control on fresh-bedrock topography under landscapes. *Proceedings of the National Academy of Sciences*, *111*(18), 6576–6581.

Riebe, C. S., Hahm, W. J., & Brantley, S. L. (2017). Controls on deep critical zone architecture: A historical review and four testable hypotheses. *Earth Surface Processes and Landforms*, *42*(1), 128–156.

Sidle, R. C., Noguchi, S., Tsuboyama, Y., & Laursen, K. (2001). A conceptual model of preferential flow systems in forested hillslopes: Evidence of self-organization. *Hydrological Processes*, *15*(10), 1675–1692.

Silliman, S. E., Berkowitz, B., Simunek, J., & Van Genuchten, M. T. (2002). Fluid flow and solute migration within the capillary fringe. *Ground Water*, *40*(1), 76–84.

Steefel, C. I., Appelo, C. A. J., Arora, B., Jacques, D., Kalbacher, T., Kolditz, O., ... Yeh, G. T. (2014). Reactive transport codes for subsurface environmental simulation. *Computational Geosciences*, *19*(3), 445–478.

Strack, O. D. L. (1984). Three-dimensional streamlines in Dupuit-Forchheimer models. *Water Resources Research*, *20*(7), 812–822.

Streltsova, T. D. (1975). Unsteady unconfined flow into a surface reservoir. *Journal of Hydrology*, *27*, 95–110.

Toth, J. (1963). A theoretical analysis of groundwater flow in small drainage basins. *Journal of Geophysical Research*, *68*(16), 4795–4812.

Troch, P. A., Berne, A., Bogaart, P., Harman, C. J., Hilberts, A. G. J., Lyon, S. W., ... Verhoest, N. E. C. (2013). The importance of hydraulic groundwater theory in catchment hydrology: The legacy of Wilfried Brutsaert and Jean-Yves Parlange. *Water Resources Research*, *49*(9), 5099–5116.

Troch, P. A., Paniconi, C., & Van Loon, E. E. (2003). Hillslope-storage Boussinesq model for subsurface flow and variable source areas along complex hillslopes: 1. Formulation and characteristic response. *Water Resources Research*, *39*(11), 331.

Troch, P., van Loon, E., & Hilberts, A. (2002). Analytical solutions to a hillslope-storage kinematic wave equation for subsurface flow. *35th Year Anniversary Issue*, *25*(6), 637–649.

Vogel, J. (1966). Investigation of groundwater flow with radiocarbon. In *Isotope Hydrology 1966 Proceedings of a Symposium*, pp. 355-369, Vienna (Austria).

Whitaker, S. (1999). *The method of volume averaging*, Theory and Applications of Transport in Porous Media. Netherlands: Springer Netherlands.

Woods, R. A., Sivapalan, M., & Robinson, J. S. (1997). Modeling the spatial variability of subsurface runoff using a topographic index. *Water Resources Research*, *33*(5), 1061–1073.

SUPPORTING INFORMATION

Additional supporting information may be found online in the Supporting Information section at the end of the article.

How to cite this article: Harman CJ, Kim M. A low-dimensional model of bedrock weathering and lateral flow coevolution in hillslopes: 1. Hydraulic theory of reactive transport. *Hydrological Processes*. 2019;1–10. https://doi.org/10.1002/hyp.13360

APPENDIX A

If the aquifer is being recharged at a spatially and temporally steady rate r, the lateral flux $Q_x(x)$ must balance the recharge being delivered from upslope of a location x (measured from the drainage divide), so $Q_x(x) = xr$.

Setting this expression for Q_x equal to Equation (3) above, gives a differential equation that can be solved if a boundary condition at the toe of the hillslope ($x = L$) can be specified. Simple cases take the form of a fixed value $H(L) = H_b$ or a fixed gradient $H'(L) = H'_b$. As noted above, the boundary condition can be important in low-relief hillslopes, but for larger relief, the boundary condition only affects the flow domain in the vicinity of the hillslope toe, and not far upslope.

When $\mathrm{Hi} = 0$ and the base is horizontal ($\theta = 0$), this gives:

$$xr = -HK\frac{\partial H}{\partial x} \tag{A1}$$

$$\text{or}\frac{\partial H^2}{\partial x} = -\frac{2r}{K}x, \tag{A2}$$

which can be solved by simply integrating and applying the boundary condition $H(L) = H_b$ to obtain (12). For the case where the base is sloping, there is not an explicit analytical solution for the steady state case. However, if we linearize (3) as suggested by Brutsaert (1994) by replacing $H(x)$ in the coefficient of the diffusive term with an effective saturated thickness $\overline{H}$:

$$Q_x = Hq_x = -K\overline{H}\frac{\partial H}{\partial x}\cos\theta + KH\sin\theta, \tag{A3}$$

a solution to the mass balance equation ($xr = Q_x$) can be found. The solution in this case can be expressed succinctly as:

$$H(x) = \frac{H_d^2}{\overline{H}\,\mathrm{Hi}^2}\left(X\,\mathrm{Hi} + 1 - e^{-\mathrm{Hi}(1-\hat{x})}(1+\mathrm{Hi})\right) + H_b e^{-\mathrm{Hi}(1-\hat{x})}, \tag{A4}$$

where:

$$H_d = L\sqrt{\frac{r}{K\cos\theta}}. \tag{A5}$$

The appropriate value of $\overline{H}$ can be found by taking the average of (A4), but this yields a cumbersome implicit solution. A good approximation is:

$$\overline{H} = \begin{cases} \sqrt{H_b^2 + \frac{2}{3}H_d^2} - \frac{1}{2}L\tan\theta & H_d < H_b \\ 0.57(H_d + H_b) & H_d > H_b. \end{cases} \tag{A6}$$

An expression for the water age can be found in the same manner as for the Hi = 0 case. In this case, although

$$T(x_0, Z) = -\frac{T^*}{\mathrm{Hi}}\left(\log Z + \psi(x_0, Z)\right), \tag{A7}$$

where $T^* = L\phi/(K\sin\theta)$ is the hillslope kinematic timescale (Berne et al., 2005), and

$$\psi = e^{-\mathrm{Hi}}\left(1 + \mathrm{Hi}\left(1 - \frac{H_b\phi}{T^* w}\right)\right)\left(\mathrm{Ei}\left(\mathrm{Hi}\frac{x}{L}\right) - \mathrm{Ei}\left(\mathrm{Hi}\frac{x_0}{L}\right)\right) - \mathrm{Hi}\frac{x - x_0}{L}. \tag{A8}$$

Ei(·) is the exponential integral function (Abramowitz & Stegun, 1964).

APPENDIX B

The 2-D advection-dispersion-reaction equation is simplified to the effective 1-D form by defining $C^*(x, Z, t) = C^*(x, z/H(x), t) = C(x, z, t)$ and taking the derivative with respect to x and z and t to obtain the substitution rules:

$$\frac{\partial C}{\partial x} \to \frac{\partial C^*}{\partial x} - Z\frac{H'(x)}{H(x)}\frac{\partial C^*}{\partial Z}, \tag{B1}$$

$$\frac{\partial C}{\partial z} \to \frac{1}{H(x)}\frac{\partial C^*}{\partial Z}, \tag{B2}$$

$$\frac{\partial^2 C}{\partial z^2} \to \frac{1}{H(x)^2}\frac{\partial^2 C^*}{\partial Z^2}, \tag{B3}$$

$$\frac{\partial C}{\partial t} \to \frac{\partial C^*}{\partial t}. \tag{B4}$$

Applying these to (1) (with lateral diffusion neglected) gives:

$$\frac{\partial(\phi C^*)}{\partial t} = -\frac{q_z - Zq_x H'(x)}{H(x)}\frac{\partial C^*}{\partial Z} + \frac{D_m}{H(x)^2}\frac{\partial^2(\phi C^*)}{\partial Z^2} + \phi R, \tag{B5}$$

if we assume $\partial C^*/\partial x = 0$. Reversing the transformation again yields (24). The new variable q_z^* is an effective flux adjusted for lateral variations in the saturated thickness:

$$q_z^* = q_z - zq_x\frac{H'(x)}{H(x)}. \tag{B6}$$

Taken in isolation, this equation makes no particular assumptions about the flux terms q_x and q_z. However, it will only be valid if the conductivity field is homogeneous or has scaled lateral symmetry. Taking the derivative of (B6) in z and substituting in (10) (the rate of change of vertical flux), we obtain (25).

Notation

- ϕ Porosity [-]
- θ The angle B is inclined from horizontal [-]
- B Base (or impermeable layer) elevation [L]
- C, C^* Solute concentration in Cartesian coordinate and in rescaled coordinate [mol/L^3]
- $\mathbf{D}$ Hydrodynamic dispersion tensor [L^2/T]
- D_m Diffusion rate [L^2/T]
- H_b Saturated thickness at the downslope boundary [L]
- H_d Maximum thickness when $H_b = 0$ and $\theta = 0$ [L]
- $H, \overline{H}$ Saturated thickness, effective saturated thickness [L]
- H' Gradient in x of saturated thickness [-]
- h Hydraulic head [L]
- $K, \overline{K}$ Hydraulic conductivity and its average in the Z dimension [L/T]
- L Hillslope length [L]
- $\vec{q} = (q_x, q_y, q_z)$ Darcy flux [L/T]
- q_z^* Effective vertical flux adjusted for lateral variations in the saturated thickness [L/T]
- r Recharge rate [L/T]
- R Solute source term [mol/L^3/T]
- t, t_0 Time, injection time [T]
- T, T^* Water age and hillslope kinematic timescale [T]
- x Horizontal coordinate (parallel to the impermeable layer) [L]
- z, z_s Vertical coordinate (orthogonal to the impermeable layer) and that of a water particle injected at x_0 at x [L]
- Z Scaled vertical coordinate [-]